

# Characterization of Cationic Polyelectrolyte-Induced Domains in Mixed POPG–POPC Lipid Bilayers via $^2\text{H}$ NMR

Kevin J. Crowell and Peter M. Macdonald\*

Department of Chemistry and Erindale College, University of Toronto, Toronto, Ontario, Canada M5S 1A2

Received: October 22, 1996; In Final Form: December 2, 1996<sup>®</sup>

The interactions of a cationic polyelectrolyte, poly(vinylbenzyltrimethylammonium chloride) (PVTA), with anionic lipid bilayer membranes composed of a mixture of phosphatidylglycerol (POPG) plus phosphatidylcholine (POPC) have been examined using  $^2\text{H}$  NMR of choline-deuterated POPC to probe membrane surface electrostatics. PVTA produces distinct membrane domains containing a 1:1 PVTA/POPG cation/anion charge ratio. The remaining PVTA-free domains are depleted with respect to POPG.

## Introduction

The interactions of polyelectrolytes with lipid bilayer membranes are of importance from both a fundamental biological and a practical biotechnical perspective. The biological significance stems from the fact that many biomolecules, such as the various polynucleic acids and proteins, are themselves polyelectrolytes. In many instances their functional mechanisms include an interaction with biological lipid bilayers. However, in most cases the molecular details of such interactions remain obscure. The biotechnical significance stems from the recent advances in the field of drug and gene therapy where lipid vesicles are used as delivery vehicles of, for example, specific gene sequences. The mechanism by which transmembrane transfer of DNA occurs remains unclear, as does the specific fate of the genetic material posttransfer.

There is extensive literature on polyelectrolyte complexation with other polyelectrolytes, with surfactants, and with proteins and DNA.<sup>1</sup> Studies of polyelectrolyte interactions with lipid bilayers are more rare but include, for example, investigations of the binding of polylysine,<sup>2,3</sup> pentyllysine,<sup>4</sup> or the cationic peptide mellitin<sup>5</sup> to anionic lipid bilayer membranes. Techniques used to study polyelectrolyte–membrane interactions include equilibrium dialysis and electrophoretic mobility measurements.<sup>6</sup> These provide information on the equilibrium and electrostatic aspects of such interactions. For instance, it can be shown that the binding of small peptides to membranes is considerably enhanced by augmenting electrostatic attraction with hydrophobic “sticker” groups covalently attached to the peptide.<sup>6</sup> Such methods yield a global picture of the polyelectrolyte–lipid bilayer complex but do not provide many important molecular details. In particular, they do not provide information regarding whether the distribution of charged species at the membrane surface is homogeneous or inhomogeneous. Recently, it has been demonstrated using fluorescence microscopy that cationic polyelectrolytes do in fact produce large scale membrane domains enriched with anionic lipids.<sup>7–9</sup> Unfortunately, the composition of the domains could not be determined in this experiment.

We describe in this report a deuterium ( $^2\text{H}$ ) NMR technique capable of determining both the degree of membrane domain formation induced by polyelectrolytes and, simultaneously, the composition of the polyelectrolyte-enriched and -depleted domains. The method is based on the ability to measure

membrane surface charge via the “molecular voltmeter” response of the head group of phosphatidylcholine, as detected in the  $^2\text{H}$  NMR spectrum of choline-deuterated POPC.<sup>10–12</sup> We investigate here the interactions of a large cationic polyelectrolyte, poly(vinylbenzyltrimethylammonium chloride) (PVTA), with lipid bilayer membranes composed of mixtures of an anionic phospholipid, 1-palmitoyl-2-oleoyl-*sn*-glycero-3-phosphoglycerol (POPG), and a zwitterionic phospholipid, 1-palmitoyl-2-oleoyl-*sn*-glycero-3-phosphocholine (POPC).

## Results and Discussion

Figure 1 shows a series of  $^2\text{H}$  NMR spectra and corresponding spectral simulations for lipid bilayers composed of mixtures of POPG + POPC- $\alpha$ - $d_2$  (40/60, mol/mol) with and without PVTA. POPC was deuterated at the  $\alpha$ - or  $\beta$ -methylene of its choline group to produce POPC- $\alpha$ - $d_2$  or POPC- $\beta$ - $d_2$ , as described in detail elsewhere.<sup>13</sup> Lipid bilayers in the form of multilamellar vesicles (MLVs) were prepared by hydrating lipids in 10 mM HEPES buffer, pH 7.4, using gentle warming and vortexing. PVTA (Scientific Polymer Products, Quebec, Canada,  $M_w$  approximately 40 000) was added during the lipid hydration step. The  $^2\text{H}$  NMR spectra were acquired at room temperature on a Chemagnetics CMX300 NMR spectrometer operating at 46 MHz for deuterium and using the quadrupole echo technique.<sup>14</sup> Other details regarding spectral acquisition are provided elsewhere.<sup>13</sup> Computer simulations of the  $^2\text{H}$  NMR spectra were produced using a spectral simulation program based on the tiling method introduced by Grant and co-workers.<sup>15</sup> The simulation permits fitting of both the quadrupolar splitting  $\Delta\nu_Q$  and the line width  $T_2$ .

The experimental spectrum on the top left in Figure 1 was acquired in the absence of PVTA. This Pake doublet spectral line shape is characteristic of liquid-crystalline lipids in a bilayer arrangement. The quadrupolar splitting  $\Delta\nu_Q$  corresponds to the separation (in Hz) between the two maxima or “horns” of the spectrum. In this case  $\Delta\nu_Q$  equals 10.2 kHz, a value greater than that measured in the absence of POPG ( $\Delta\nu_Q = 6.3$  kHz for 100% POPC- $\alpha$ - $d_2$ ) by an amount which is proportional to the POPG content (40 mol %). The corresponding spectral simulation, shown on the right, consists of a single spectral component, indicating that all the POPC molecules in the entire MLV preparation experience an identical surface charge environment.

The middle spectrum on the left in Figure 1 was obtained when PVTA was added in an amount such that the PVTA/POPG cation/anion charge ratio equals 0.667. Two quadrupolar

\* To whom correspondence should be addressed. Tel: 905-828-3805. Fax: 905-828-5425. E-mail: pmacdona@credit.erin.utoronto.ca.

<sup>®</sup> Abstract published in *Advance ACS Abstracts*, January 1, 1997.

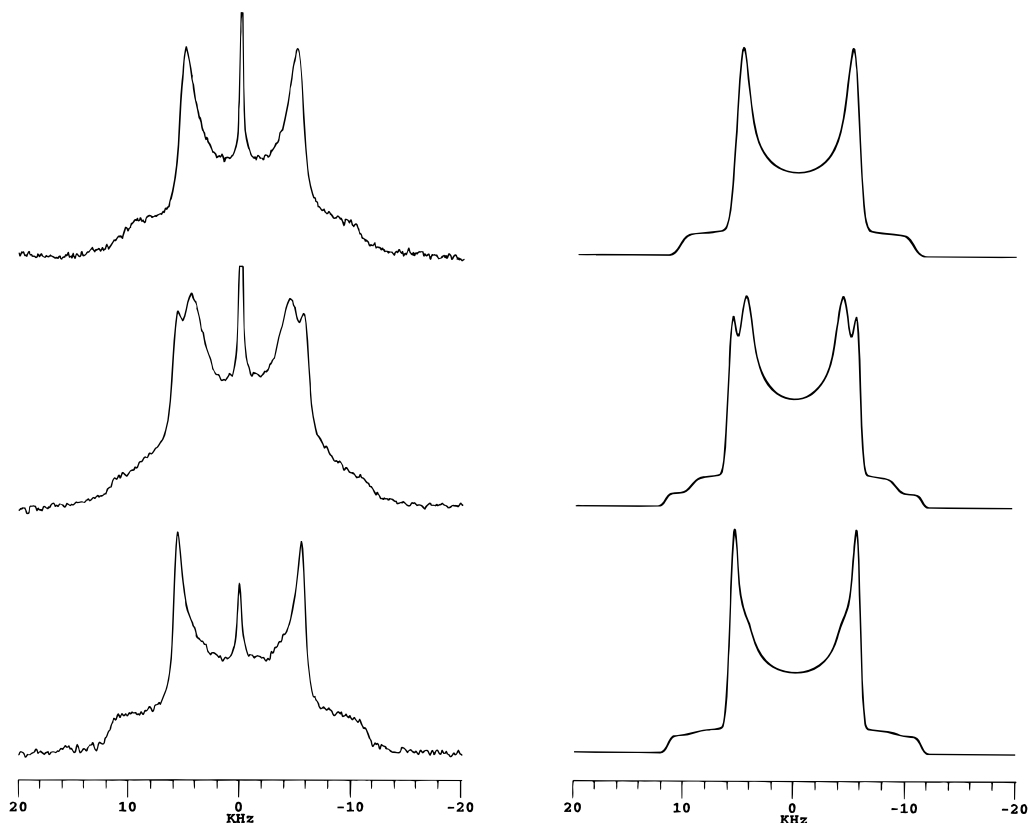


**Figure 1.**  $^2\text{H}$  NMR spectra (left) and corresponding spectral simulations (right) for POPG + POPC- $\alpha$ - $d_2$  (40/60, mol/mol) with, from top to bottom, 0, 0.667, and 1.0 PVTA/POPG.

splittings are clearly evident. One is greater than, and one is less than, the value obtained in the absence of PVTA. The corresponding spectral simulation on the right requires the superposition of two Pake doublets of roughly equal integrated intensity but different  $\Delta\nu_Q$  and  $T_2$ . Relaxation time measurements (data not shown) indicate that the spectral component with the smaller  $\Delta\nu_Q$  exhibits a  $T_2$  identical to that of the control spectrum, while the spectral component with the larger  $\Delta\nu_Q$  displays a  $T_2$  which is 50% longer.

The bottom spectrum on the left in Figure 1 was obtained with a PVTA/POPG cation/anion charge ratio equal to 1.0. It is dominated by a single spectral component with  $\Delta\nu_Q$  equal to that of the larger  $\Delta\nu_Q$  component in the middle spectrum. It is possible to simulate this spectrum by including a small contribution from a spectral component with  $\Delta\nu_Q$  equal to that of the smaller  $\Delta\nu_Q$  component in the middle spectrum, as shown on the right, but the uncertainty in its relative intensity is considerable.

Figure 2 shows the corresponding experimental  $^2\text{H}$  NMR spectra and spectral simulations for the case of POPG + POPC- $\beta$ - $d_2$  (30/70) with and without PVTA. The experimental spectrum on the top left was acquired in the absence of PVTA and has  $\Delta\nu_Q$  equal to 2.7 kHz. This is reduced relative to the value of 5.8 kHz measured for 100% POPC- $\beta$ - $d_2$  by an amount which is proportional to the POPG content (30 mol %). Note that the perturbation in  $\Delta\nu_Q$  produced by the anionic phospholipid POPG is opposite in sense for POPC- $\alpha$ - $d_2$  versus POPC- $\beta$ - $d_2$ . This counterdirectional change in  $\Delta\nu_Q$  is characteristic of the "molecular voltmeter" response to surface charge and indicates that the choline head group of POPC undergoes a concerted conformational change in response to surface charges.<sup>10–12</sup> In this case the direction of the change is diagnostic of the presence of anionic charge from POPG.

The middle spectrum in Figure 2 was obtained upon adding PVTA in an amount such that the PVTA/POPG cation/anion

charge ratio equals 0.40. Two quadrupolar splittings are again evident, one being greater than, and one less than, the value obtained in the absence of PVTA. The corresponding spectral simulation again requires the superposition of two Pake doublets of roughly equal integrated intensity and  $T_2$  but different  $\Delta\nu_Q$ .

The bottom spectrum in Figure 2 was obtained with a PVTA/POPG cation/anion charge ratio equal to 1.0. It is dominated by a single spectral component with  $\Delta\nu_Q$  equal to that of the smaller  $\Delta\nu_Q$  component in the middle spectrum. It is possible to simulate this spectrum by including a small contribution from a spectral component with  $\Delta\nu_Q$  equal to that of the larger  $\Delta\nu_Q$  component in the middle spectrum, but, as was the case with POPC- $\alpha$ - $d_2$ , the uncertainty in its intensity is considerable.

Figure 3 summarizes the intensities (part A) and the quadrupolar splittings (part B) of the two spectral components in the POPC- $\alpha$ - $d_2$  and POPC- $\beta$ - $d_2$   $^2\text{H}$  NMR spectra for different PVTA/POPG cation/anion charge ratios. For the case of POPC- $\alpha$ - $d_2$  in POPG + POPC (40/60) bilayers, the spectral component with the larger  $\Delta\nu_Q$  increases in intensity with increasing PVTA, while that with the smaller  $\Delta\nu_Q$  decreases. Identical results are obtained for POPC- $\beta$ - $d_2$  except it is the spectral component with the smaller  $\Delta\nu_Q$  which increases in intensity with increasing PVTA.

The linear dependence on the PVTA/POPG cation/anion charge ratio indicates that these two spectral components correspond to polyelectrolyte-bound and polyelectrolyte-free POPC populations in slow exchange with one another on a time scale delimited by the difference in their quadrupolar splittings. The fact that the quadrupolar splittings from POPC- $\alpha$ - $d_2$  versus POPC- $\beta$ - $d_2$  change in opposite directions in both the PVTA-bound and the PVTA-free domains indicates that these two environments differ with respect to their surface charge. In Figure 3B one observes that  $\Delta\nu_Q$  from POPC- $\alpha$ - $d_2$  in the PVTA-bound domain remains virtually constant across a range of PVTA/POPG ratios, while  $\Delta\nu_Q$  from POPC- $\alpha$ - $d_2$  in the PVTA-

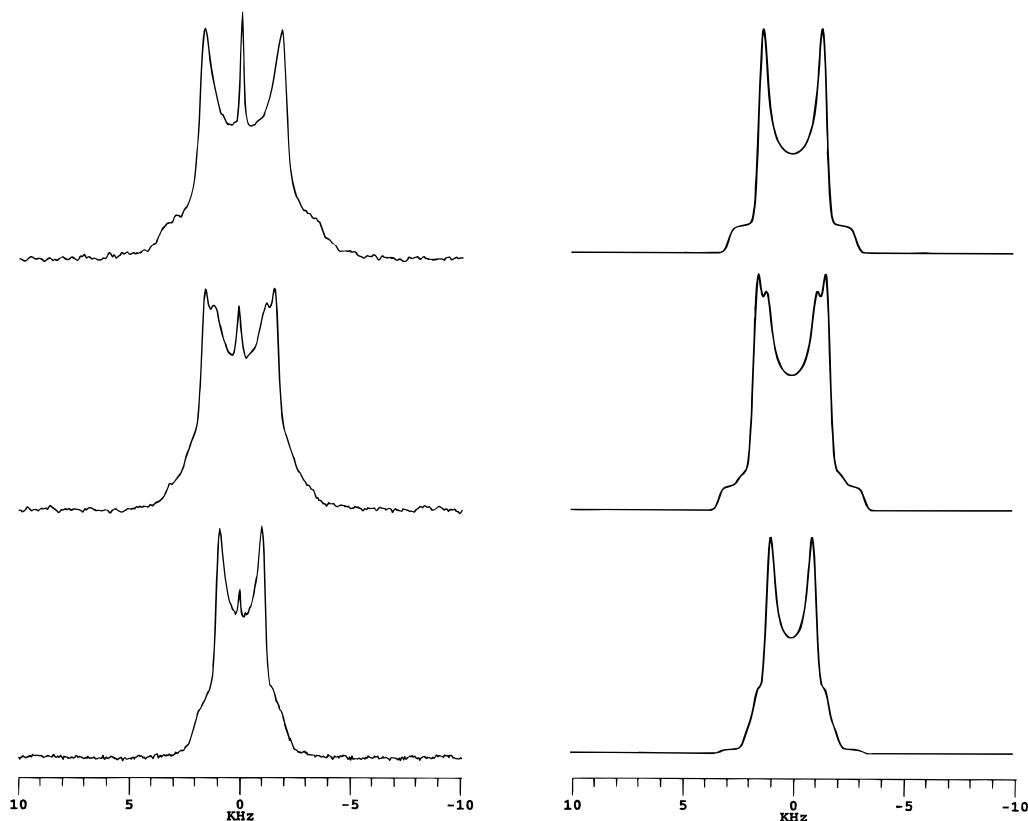


**Figure 2.**  $^2\text{H}$  NMR spectra (left) and corresponding spectral simulations (right) for POPG + POPC- $\beta$ - $d_2$  (30/70, mol/mol) with, from top to bottom, 0, 0.40, and 1.0 PVTA/POPG.

free domain decreases progressively. This suggests a more-or-less constant surface charge environment within the PVTA-bound domain coupled to a PVTA-free domain which becomes progressively depleted with respect to POPG as further PVTA is added. The overall effect is less apparent for the case of POPC- $\beta$ - $d_2$ , but this difference cannot be attributed to any inherent difference in the sensitivity of POPC- $\alpha$ - $d_2$  versus POPC- $\beta$ - $d_2$  to POPG levels. It may be due to the fact that 40 mol % POPG was used for the case of POPC- $\alpha$ - $d_2$  while 30 mol % POPG was used for the case of POPC- $\beta$ - $d_2$ . This point is currently under investigation.

We have also carried out  $^{31}\text{P}$  NMR measurements on identical MLVs with and without PVTA. The  $^{31}\text{P}$  NMR line shape is sensitive to the macroscopic architecture of the phospholipids and, therefore, detects the presence of bilayer versus nonbilayer lipid arrangements such as isotropic, or cubic, or hexagonal  $\text{H}_{\text{II}}$  lipid phases.<sup>16,17</sup> In every case the  $^{31}\text{P}$  NMR line shape was characteristic of liquid-crystalline phospholipids in a bilayer arrangement (data not shown).

The  $^2\text{H}$  NMR results demonstrate that the interaction of PVTA with a lipid bilayer surface produces a separate domain, having a distinct composition, but retaining an overall liquid-crystalline bilayer architecture. It is highly improbable that the observed domains result from a macroscopic separation of lipid vesicle populations differing in the amount of bound polyelectrolyte, since the global polyelectrolyte to lipid vesicle ratio is typically on the order of 10 000 to 1. Instead, the observed domains are most likely due to lateral segregation of lipids within the plane of a given lipid bilayer.

The composition of the two domains may be determined from an analysis of the  $^2\text{H}$  NMR quadrupolar splittings. The POPG content of the PVTA-free domain is calculated using eq 1

$$\frac{x_z^f(\Delta\nu^f - \Delta\nu_0)}{(m_- - \Delta\nu^f + \Delta\nu_0)} = X_-^f \quad (1)$$

where  $\Delta\nu^f$  is the quadrupolar splitting of either POPC- $\alpha$ - $d_2$  or POPC- $\beta$ - $d_2$  in that domain,  $\Delta\nu_0$  is the quadrupolar splitting for 100% POPC,  $m_-$  is a calibration constant relating  $\Delta\nu_Q$  to the POPG content,  $X_z^f$  is the fraction of the total POPC in the PVTA-free domain as determined by spectral simulation (and illustrated in Figure 3A), and  $X_-^f$  is the fraction of the total POPG in the PVTA-free domain.<sup>18</sup> For POPG,  $m_-$  equals +9.6 kHz/mol and -8.4 kHz/mol for POPC- $\alpha$ - $d_2$  and POPC- $\beta$ - $d_2$ , respectively.<sup>19</sup> Equation 1 is valid for the case of a binary mixture of anionic plus zwitterionic lipids, where there is a linear relationship between the mole fraction of charged lipid and the quadrupolar splitting. These conditions pertain to the PVTA-free domain. Applying this analysis to the data in Figure 3B reveals that the PVTA-free domain is progressively depleted with respect to POPG as increasing amounts of PVTA are added. One may then calculate the corresponding enrichment of the PVTA-bound domain with respect to POPG. For every PVTA/POPG level investigated, regardless of whether one employs quadrupolar splittings obtained with POPC- $\alpha$ - $d_2$  or POPC- $\beta$ - $d_2$ , one calculates that the PVTA-bound domain contains a 1:1 ratio of PVTA cationic charges to POPG anionic charges.

One of the most interesting aspects of these systems is that the polyelectrolyte itself does not appear to interact directly with POPC. Rather its presence is sensed by the molecular voltmeter only indirectly through its effects on the local POPG concentration. In a ternary mixture of cationic + anionic + zwitterionic species, we expect the observed  $\Delta\nu_Q$  to be perturbed relative to the value measured for 100% POPC by an amount which is the sum of the perturbations due to the cationic and anionic species individually in binary mixtures.<sup>20</sup> This should cause  $\Delta\nu_Q$  to return toward a value characteristic of a neutral surface.

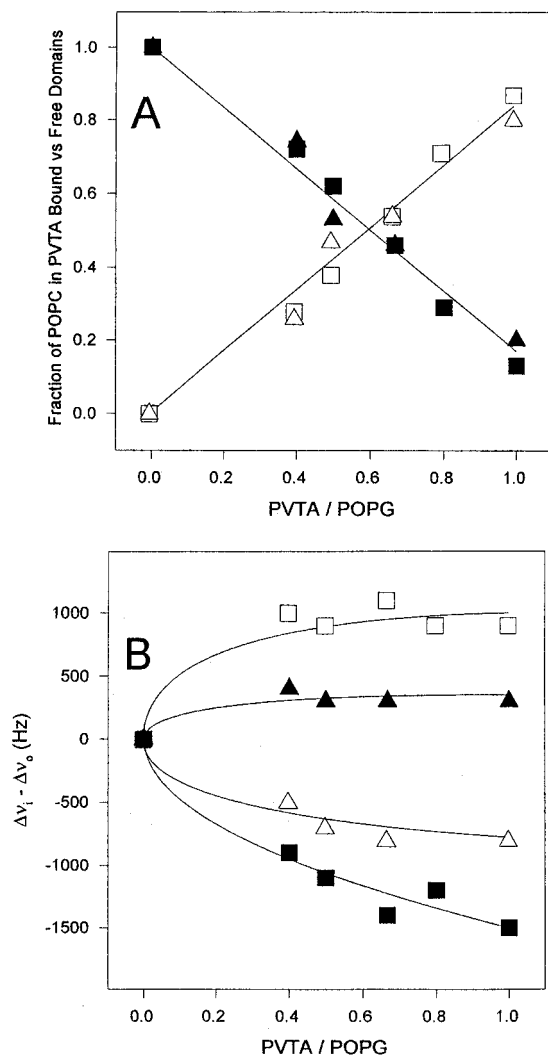


**Figure 3.** (A) Relative intensities of the POPC fractions in the PVTA-bound (open symbols) and PVTA-free (closed symbols) domains derived from simulations of the  $^2\text{H}$  NMR spectra of mixtures of POPG + POPC- $\alpha$ - $d_2$  (40/60, mol/mol) (squares) or POPG + POPC- $\beta$ - $d_2$  (30/70, mol/mol) (triangles). (B) Quadrupolar splittings of the POPC fractions in the PVTA-bound (open symbols) and PVTA-free (closed symbols) domains measured from the  $^2\text{H}$  NMR spectra of mixtures of POPG + POPC- $\alpha$ - $d_2$  (40/60, mol/mol) (squares) or POPG + POPC- $\beta$ - $d_2$  (30/70, mol/mol) (triangles).

Instead,  $\Delta\nu_Q$  for the PVTA-bound domain is characteristic of an enrichment with POPG! If one assumes the PVTA is not sensed directly by the molecular voltmeter, then one may calculate the POPG content of the PVTA-bound domain from the observed  $\Delta\nu_Q$  using an expression analogous to eq 1. One discovers that the enrichment with POPG calculated in this fashion for the PVTA-bound domain exactly matches the POPG depletion of the PVTA-free domain. One scenario in which POPC would be unable to interact directly with PVTA would be that in which the polyelectrolyte was "masked" by a coating of POPG acting as counterions. Similar observations have been made in the electrostatic mirror-image experiment in which anionic polyadenosine interacts with lipid bilayers containing synthetic cationic amphiphiles.<sup>18</sup>

A hypothetical picture of PVTA's configuration when bound to a lipid bilayer membrane is shown in Figure 4. We hypothesize that in this regard PVTA resembles a polynucleic acid. NMR<sup>21</sup> and infrared<sup>22</sup> evidence indicates that polynucleic acids bind to lipid bilayers such that their aromatic bases penetrate into the acyl chain region, leaving the sugar-phosphate backbone located within the polar interface region.

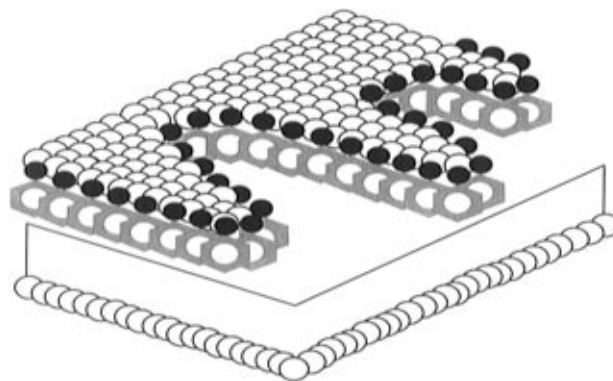


**Figure 4.** Schematic representation of a PVTA polyelectrolyte at a lipid bilayer membrane surface. The lipophilic polymer backbone and benzyl side chains intercalate between the lipids, while the hydrophilic trimethyl amino group remains proximal to the aqueous interface. The polyelectrolyte adopts an extended random-coil configuration in two-dimensions. In the region defined by proximity to the PVTA the PVTA/POPG cation/anion charge ratio is 1:1. POPC trapped within this region experiences restricted diffusion and cannot readily exchange with the bulk bilayer lipid.

PVTA resembles a polynucleic acid in that it is composed of aromatic ring side chains pendant from a polymeric backbone, with charged groups topologically sequestered into a distinct region of the polymer. In polynucleic acids the charged moieties are located exclusively on the sugar-phosphate backbone, while in PVTA they are located at the para position of the phenyl ring. Thus, the hydrophobic polymer backbone and benzene ring side chains of PVTA could intercalate between the membrane lipids, driven by the need to minimize their interactions with water. Also, PVTA's cationic trimethylamino groups could reside at the membrane-water interface in order to maximize their interactions with the anionic phosphate groups of POPG. The conformation of the PVTA would probably be best described in terms of a self-avoiding random walk in two dimensions. POPG remains in the vicinity of the PVTA due to electrostatic attraction such that there is a 1:1 ratio of PVTA cationic to POPG anionic charges in the region defined by proximity to the polyelectrolyte. POPC may be trapped within the folds of the PVTA where its effective lateral diffusion coefficient is reduced due to the well-known archipelago effect.<sup>23</sup> This inhibits POPC's ability to exchange with the bulk lipid but does not prevent other molecular motions. At present this picture of PVTA bound to lipid bilayers is purely hypothetical but does provide a point of departure for further studies.

The size of the PVTA-bound domain may be estimated by summing the cross-sectional areas occupied at the membrane surface by the phospholipids and the polyelectrolyte. Individual POPC and POPG molecules occupy surface areas of  $68 \text{ \AA}^2$ . An estimate of the area occupied by the polyelectrolyte is obtained by regarding it as a chain of length  $190 \times 3.55 \text{ \AA}$  and width  $2.42 \text{ \AA}$ , where 190 is the number of monomers per chain,  $3.55 \text{ \AA}$  is the monomer-monomer spacing, and  $2.42 \text{ \AA}$  is the width of a benzene ring. For the case of POPG + POPC (40/60), the  $^2\text{H}$  NMR data indicate that each PVTA domain contains approximately 190 POPG plus 200 POPC molecules per PVTA molecule, yielding a total area equivalent to a circular area with a radius of  $93 \text{ \AA}$ . This is far less than the dimensions of a fully-extended PVTA chain ( $675 \text{ \AA}$ ) but far greater than the dimensions of a fully-collapsed PVTA chain ( $23 \text{ \AA}$ ). According to De Gennes,<sup>24</sup> the dimensions of an ideal polymer confined to two-dimensions should scale with molecular weight as  $M^{3/5}$ . Using the  $^2\text{H}$  NMR technique described here, this scaling law is now amenable to investigation for the case of polyelectrolytes bound at a lipid membrane surface. It is interesting that the

domain size defined by a single polyelectrolyte, as estimated above, is too small to account for the observation of distinct domains in the  $^2\text{H}$  NMR spectrum, assuming that the diffusion coefficient of a lipid within the domain equals that measured in a bulk lipid bilayer ( $D_0 = 5 \times 10^{-12} \text{ m}^2 \text{ s}^{-1}$ <sup>25</sup>) and applying the two-dimensional Einstein equation with a diffusion time corresponding to the echo time in the quadrupolar echo pulse sequence (50  $\mu\text{s}$ ). This implies that either the lipid diffusion coefficient within the polyelectrolyte-bound domain is much less than that in the bulk or the individual polyelectrolyte-bound domains have aggregated into much larger domains. Both possibilities seem likely.<sup>23,7-9</sup>

**Acknowledgment.** This research was supported by an Operating Grant (P.M.M.) from the National Science and Engineering Research Council of Canada.

## References and Notes

- (1) Dubin, P.; Bock, J.; Davis, R.; Schulz, D.; Thies, C., Eds. *Macromolecular Complexes in Chemistry and Biology*, Springer-Verlag: New York, 1994.
- (2) De Kruijff, B.; Cullis, P. R. *Biochim. Biophys. Acta.* **1980**, 601, 235.
- (3) De Kruijff, B.; Rietveld, A.; Tolders, N.; Vaandrager, B. *Biochim. Biophys. Acta.* **1985**, 820, 295.
- (4) Roux, M.; Neumann, J.-M.; Bloom, M.; Devaux, P. F. *Eur. Biophys. J.* **1988**, 16, 267.
- (5) Beschiaschvili, G.; Seelig, J. *Biochemistry* **1990**, 29, 52.
- (6) McLaughlin, S.; Aderem, A. *Trends Biochem. Sci.* **1995**, 20, 272.
- (7) Luan, P.; Glaser, M. *Biochemistry* **1994**, 33, 4483.
- (8) Yang, L.; Glaser, M. *Biochemistry* **1995**, 34, 1500.
- (9) Luan, P.; Yang, L.; Glaser, M. *Biochemistry* **1995**, 34, 9874.
- (10) Seelig, J.; Macdonald, P. M. *Acc. Chem Res.* **1987**, 20, 221.
- (11) Seelig, J.; Macdonald, P. M.; Scherer, P. G. *Biochemistry* **1987**, 26, 7535.
- (12) Scherer, P. G.; Seelig, J. *Biochemistry* **1989**, 28, 7720.
- (13) Marassi, F. M. Ph.D. Thesis, University of Toronto, 1993.
- (14) Davis, J. H.; Jeffrey, K. R.; Bloom, M.; Valic, M. I.; Higgs, T. P. *Chem. Phys. Lett.* **1976**, 42, 390.
- (15) Alderman, D. W.; Solum, M. S.; Grant, D. M. *J. Chem. Phys.* **1986**, 84, 3717.
- (16) Seelig, J. *Biochim. Biophys. Acta* **1978**, 515, 105.
- (17) Cullis, P. R.; De Kruijff, B. *Biochim. Biophys. Acta* **1979**, 559, 399.
- (18) Mitrakos, P.; Macdonald, P. M. *Biochemistry* **1996**, 35, 16714.
- (19) Macdonald, P. M.; Liesen, J.; Marassi, F. M. *Biochemistry* **1991**, 30, 3558.
- (20) Marassi, F. M. Macdonald, P. M. *Biochemistry* **1992**, 31, 10031.
- (21) Budker, V. G.; Merkushin, Y. A. *Biol. Membr.* **1990**, 7, 419.
- (22) Mal'tseva, T. V.; Bichenkov, E. E.; Budker, V. G. *Biofizika* **1983**, 28, 55.
- (23) Saxton, M. J. *Biophys. J.* **1993**, 56, 1053.
- (24) De Gennes, P. *Scaling Concepts in Polymer Physics*; Cornell University Press, London, 1979.
- (25) Lindblom, G.; Oräd, G. *Prog. Nucl. Magn. Reson. Spectrosc.* **1994**, 26, 483.